A Diffusion–Translocation Model for Gradient Sensing by Chemotactic Cells

Marten Postma and Peter J. M. Van Haastert
Groningen Biomolecular Sciences and Biotechnology Institute, Department of Biochemistry, University of Groningen, Nijenborgh 4, 9747 AG Groningen, The Netherlands

ABSTRACT Small chemotactic cells like *Dictyostelium* and neutrophils transduce shallow spatial chemoattractant gradients into strongly localized intracellular responses. We show that the capacity of a second messenger to establish and maintain localized signals, is mainly determined by its dispersion range, $\lambda = \sqrt{D_m/k_{-1}}$, which must be small compared to the cell's length. Therefore, short-living second messengers (high k_{-1}) with diffusion coefficients D_m in the range of 0–5 $\mu m^2\ s^{-1}$ are most suitable. Additional to short dispersion ranges, gradient sensing may include positive feedback mechanisms that lead to local activation and global inhibition of second-messenger production. To introduce the essential nonlinear amplification, we have investigated models in which one or more components of the signal transduction cascade translocate from the cytosol to the second messenger in the plasma membrane. A one-component model is able to amplify a 1.5-fold difference of receptor activity over the cell length into a 15-fold difference of second-messenger concentration. Amplification can be improved considerably by introducing an additional activating component that translocates to the membrane. In both models, communication between the front and the back of the cell is mediated by partial depletion of cytosolic components, which leads to both local activation and global inhibition. The results suggest that a biochemically simple and general mechanism may explain various signal localization phenomena not only in chemotactic cells but also those occurring in morphogenesis and cell differentiation.

INTRODUCTION

Many biochemical and cellular processes, such as nuclear division, lipid transport, and cytoskeletal rearrangement are nonuniformly distributed within the cell. A pronounced example is chemotaxis, a process where cells move in the direction of a chemical gradient. Prokaryotic cells detect a temporal change in chemoattractant concentration and change the duration of movement depending on whether they move toward or away from the chemotactic source (Stock and Mowbray, 1995; Stock et al., 1989). However, eukaryotic cells detect a spatial difference of chemoattractant by measuring the difference in concentration between the ends of the cell, and then they move up the gradient of chemoattractant (Devreotes and Zigmond, 1988). Examples are human neutrophils that react to small peptides, such as fMLP, *Dictyostelium* that responds to cAMP, and platelet-derived growth factor (PDGF) that induces directional movement of fibroblasts in wound-healing processes (Heldin and Westermark, 1999).

Activation of receptors in the plasma membrane induces production of second-messenger molecules that, by diffusion, transduce the signal to structures that initiate pseudopod formation. However, diffusion of second-messenger molecules will also lead to signal dispersion: loss of spatial information. The diffusion speed of second-messenger molecules can be very different and mainly depends on their size and location. The observed value may, however, differ considerably if molecules bind to immobile structures (cytoskeleton or large protein complexes) or if obstacles restrict their path. Small soluble molecules, like cAMP, cGMP, Ca^{2+}, and IP_3, generally have diffusion coefficients well above 100 $\mu m\ s^{-1}$ (see, for example, Chen et al., 1999; Allbritton et al., 1992), whereas small membrane-bound molecules like DAG and PIP_3 diffuse at least 100-fold slower because the diffusion coefficients are in the order of 1 $\mu m^2\ s^{-1}$ (see Almeida and Vaz, 1995; Korlach et al., 1999). The diffusion coefficients of free cytosolic proteins are in the order of 10–50 $\mu m^2\ s^{-1}$ (see Arrio-Dupont et al., 2000), depending on their size, and those of membrane-bound proteins are ~0.1 $\mu m^2\ s^{-1}$ (see Niv et al., 1999). An equally important factor in signal dispersion is the second messenger's lifetime. In contrast to long lifetimes, second messengers with short lifetimes preserve spatial information much better (Haugh et al., 2000). In addition to formation of second-messenger molecules, receptor activation may also lead to translocation of cytosolic proteins to docking sites in the plasma membrane generated by the activated receptors. Such docking sites may include phosphorylated tyrosines on growth-factor receptors that bind Src homology 2 (SH2) domain-containing proteins, or phosphatidyl inositol phospholipids that bind proteins with a pleckstrin homology (PH) domain (Teruel and Meyer, 2000).

Because cells are able to sense very weak gradients of chemoattractant, the transduction mechanism must be able to convert a difference in receptor occupancy between front and back of the cell in an all-or-nothing response at the front. Asymmetric amplification of the signal between front

Received for publication 11 January 2001 and in final form 24 May 2001.
Address reprint requests to Peter J. M. Van Haastert, GBB, Dept. of Biochemistry, University of Groningen, Nijenborgh 4, 9747 AG Groningen, The Netherlands. Tel.: +31-503634172; Fax +31-503634165; E-mail: P.J.M.van.Haastert@chem.rug.nl.

0006-3495/01/09/1314/10 $2.00

and back of the cell is essential to transduce weak spatial information. Thus, two major events have to be understood: diffusion/degradation of second-messenger molecules for spatial intracellular communication, and nonlinear amplification to convert weakly localized signals into strongly localized responses. In this study, we have investigated the fundamental role of diffusion and degradation of second-messenger molecules in gradient-sensing mechanisms. Based on translocation experiments (Parent et al., 1998; Firtel and Chung, 2000; Servant et al., 2000; Haugh et al., 2000) and activator-inhibitor models (Meinhardt, 1999; Meinhardt and Gierer, 2000; Haugh and Lauffenburger, 1997), we propose a diffusion–translocation model that may provide the required amplification in gradient sensing.

MATERIALS AND METHODS

We assume that the proteins synthesizing the second messengers are immobile and are located in or at the membrane, and are activated by local receptors. After its production, a second-messenger molecule will diffuse from its location of synthesis, either into the cytosol or laterally in the membrane, and, ultimately, it will be degraded. This general reaction–diffusion process is described by (see, for example, Haugh et al., 2000)

$$\frac{\mathrm{d}m}{\mathrm{d}t} = D_\mathrm{m}\nabla^2 m - k_{-1}m + P, \qquad (1)$$

where m is the position-dependent second-messenger concentration (with unit μM for cytosolic molecules or molecules $\cdot\ \mu\mathrm{m}^{-2}$ for membrane molecules), D_m the diffusion coefficient of the second messenger, k_{-1} the degradation rate constant, and P the production rate (unit: $\mu\mathrm{Ms}^{-1}$ or molecules$\mu\mathrm{m}^{-2}\ \mathrm{s}^{-1}$ for cytosolic and membrane-bound second messengers, respectively). We have studied solutions of Eq. 1 for different cases of cell geometry and production, diffusion, and degradation rates. All calculations where done numerically and, when possible, also with analytical solutions. The solutions of Eq. 1 were derived by the Laplace transform method as described in Carslaw and Jaeger (1959) and Crank (1979). We discuss two cases where analytical solutions of Eq. 1 exist.

A point source of second-messenger production

We assume that second-messenger production takes place at a constant rate $p = k_\mathrm{P}$ at one end face of a cylinder with length L, and that degradation and diffusion occurs along the axial coordinate of the cylinder. When second-messenger production starts at $t = 0$, i.e., $m(x, 0) = 0$, the solution of Eq. 1 is

$$m(x,t) = \frac{k_\mathrm{P}}{k_{-1}}\frac{L}{\lambda}\frac{\cosh((L-x)/\lambda)}{\sinh(L/\lambda)} - k_\mathrm{P}\sum_{\mathrm{n}=-\infty}^{\infty}\tau_\mathrm{n}\cos\left(n\pi\frac{x}{L}\right)e^{-\mathrm{t}/\tau_\mathrm{n}}, \qquad (2)$$

where $0 < x < L$; the space constant λ is given by $\lambda = \sqrt{D_\mathrm{m}/k_{-1}}$ and the time constants τ_n by $\tau_\mathrm{n} = 1/(k_{-1} + n^2\pi^2 D_\mathrm{m}/l^2)$. The first term in Eq. 2 is the steady-state solution and will be reached quickly when the time constants are small, i.e., at high degradation rates (k_{-1}), fast diffusion (D_m) and in small cells (L).

A gradient of second-messenger production

We next consider a spherical cell, with radius r, where production, diffusion, and degradation of the second messenger occur at the inner face of the cell membrane. We assume that an external gradient of chemoattractant induces a linear gradient in receptor activity along the x-coordinate; $-r \le x \le r$. This linear gradient of receptor activity is given by

$$R^*(x) = \bar{R}^* - \Delta R^*\frac{x}{r}, \qquad (3)$$

where $R^*(x)$ is the local fraction of active receptors, $\bar{R}^* = (R^*_\mathrm{f} + R^*_\mathrm{b})/2$ represents the mean fraction of active receptors and $\Delta R^* = (R^*_\mathrm{f} - R^*_\mathrm{b})/2$ represents the difference between the ends of the cell in the fraction of active receptors. The maximum production rate, k_R, will be reached when all receptors are active, and, hence, the local production rate of second messenger is given by $P(x) = k_\mathrm{R}R^*(x)$.

The time and space dependence of the second-messenger concentration then follows from Eq.1 with the initial condition $m(x, 0) = 0$:

$$m(x,t) = \frac{k_\mathrm{R}}{k_{-1}}\left(\bar{R}^* - F\Delta R^*\frac{x}{r}\right) - \frac{k_\mathrm{R}}{k_{-1}}\left(\bar{R}^* e^{-\mathrm{t}/\varepsilon_0} - F\Delta R^*\frac{x}{r}e^{-\mathrm{t}/\varepsilon_1}\right), \qquad (4)$$

where the factor $F = r^2/(2\lambda^2 + r^2)$, and the time constants are $\varepsilon_0 = 1/k_{-1}$ and $\varepsilon_1 = 1/(k_{-1} + 2D_\mathrm{m}/r^2)$, respectively. The time-independent part of Eq. 4 is the steady-state solution.

The concentration of second messenger in the sphere's volume can also be derived from Eq. 1. The resulting expression for the steady-state solution for the concentration just below the surface is similar to that of Eq. 4, but more complex.

RESULTS

Second-messenger gradient formation under point-source production

When a second messenger is produced at a certain cellular location, how far and how fast will it diffuse from this point source, given a specific diffusion coefficient and degradation rate? To illustrate the main factors determining the fate of a signal, we first consider the idealized case of a cylindrically shaped cell. We assume that second-messenger production takes place at only one end face and that degradation occurs throughout the cell (Fig. 1, *inset*). When the production of second messenger at the cylinder front face starts at $t = 0$, the space–time dependence of the second-messenger concentration is described by a two-dimensional reaction–diffusion equation, which has solution Eq. 2. In this equation, the space constant $\lambda = \sqrt{D_\mathrm{m}/k_{-1}}$ determines the dispersion range of the second messenger. For long cells, about 95% of the molecules are localized within a distance of 3λ from the source.

In a cell with typical length $L = 10\ \mu$m, the steady-state concentration profiles were calculated for three values of the diffusion coefficient: $D_\mathrm{m} = 1\ \mu\mathrm{m}^2\ \mathrm{s}^{-1}$, a typical value for membrane phospholipids or very large cytosolic proteins; $D_\mathrm{m} = 10\ \mu\mathrm{m}^2\ \mathrm{s}^{-1}$, typical for cytosolic proteins; and $D_\mathrm{m} = 100\ \mu\mathrm{m}^2\ \mathrm{s}^{-1}$, characteristic for cAMP. The values

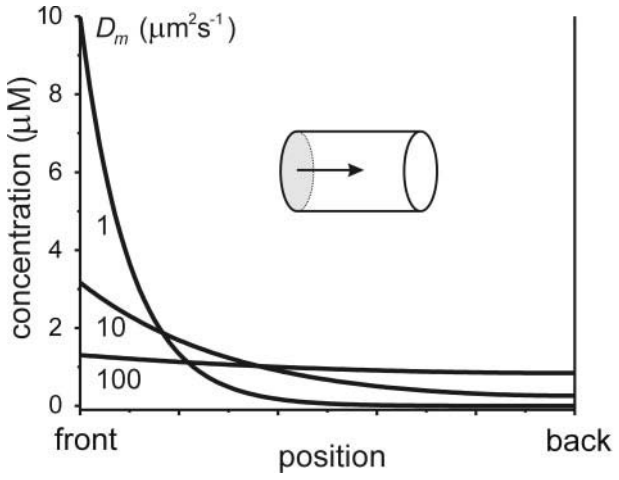

FIGURE 1 Diffusion of second messenger produced at one face of a cylindrical cell. Concentration profiles of second messenger in the steady state for different diffusion coefficients D_m; $L = 10$ μm and $k_{-1} = 1.0\ s^{-1}$. Slow diffusion leads to a localized signal and fast diffusion leads to dispersal of the gradient.

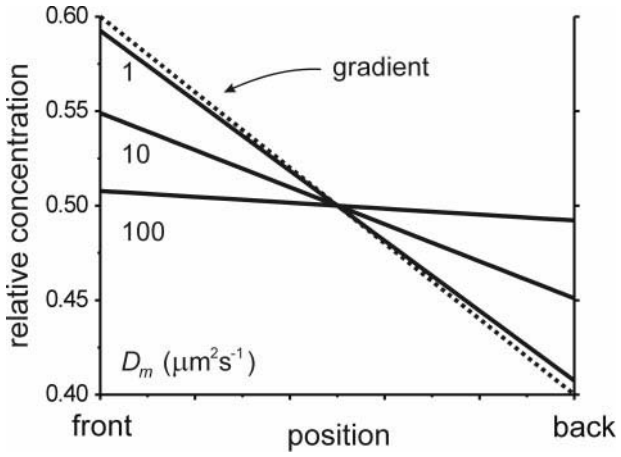

FIGURE 2 Diffusion of second messenger produced as a gradient in a spherical cell. Steady-state second-messenger concentration profiles at or just below the cell's surface were calculated for different diffusion coefficients using a 60–40% gradient of receptor activity (*dotted line*), a degradation rate of $k_{-1} = 1.0\ s^{-1}$ and radius $r = 5$ μm. The data are normalized to 0.5 at the center of the cell. Diffusion leads to dissipation of the gradient. The gradient is almost completely lost with a fast-diffusing molecule ($D_m = 100\ \mu m^2\ s^{-1}$), while the intracellular gradient becomes increasingly proportional to the receptor activity gradient at $D_m = 1\ \mu m^2\ s^{-1}$.

taken for the degradation rate and the second-messenger production rate were $k_{-1} = 1\ s^{-1}$ and $k_P = 1\ \mu Ms^{-1}$, respectively (Fig. 1). A diffusion coefficient of $D_m = 1\ \mu m^2\ s^{-1}$ yields a space constant of $\lambda = 1$ μm. The concentration of the second messenger is very high near the place of production and falls off steeply to zero values at a few micrometer away from the source. For $D_m = 10\ \mu m^2\ s^{-1}$ ($\lambda = 3.3$ μm), the second-messenger concentration in the steady state still exhibits a noticeable gradient, but with a diffusion coefficient of $D_m = 100\ \mu m^2\ s^{-1}$ ($\lambda = 10$ μm), the concentration profile is nearly flat. Because production and degradation rates are kept constant, the total amount of second-messenger molecules in the cell is the same in all three cases.

The effect of second messenger degradation on signal localization is complementary to that of diffusion speed, due to the space constant $\lambda = \sqrt{D_m/k_{-1}}$. A lower degradation rate will lead to stronger dispersal of signals in the cell, and also to a larger total concentration, i.e., stronger signals. In contrast, high degradation rates will lead to more localized signals, but unavoidably the total concentration will decrease. To overcome a lower concentration, the production rate must be increased accordingly. The results show that, to allow the formation of a steep gradient, the space constant λ must be ≤1 μm. Thus, gradient transduction by a second messenger such as cAMP with a diffusion coefficient over $100\ \mu m^2\ s^{-1}$ requires a degradation rate above $100\ s^{-1}$, implying a half-life below 10 ms.

Receptor-coupled second-messenger production in chemoattractant gradients

In *Dictyostelium* cells, receptor molecules are probably uniformly distributed around the cell's periphery (Xiao et al., 1997). Because chemoattractant molecules can reversibly bind to the receptors, the fraction of active receptors depends on the local chemoattractant concentration. We assume that the activated receptors locally couple to effector enzymes that then produce second-messenger molecules at the inner face of the plasma membrane. The subsequent diffusion/degradation of second messenger will take place at the cell's inner surface (i.e., the plasma membrane in the case of phospholipid second messenger) or in the cell's volume (i.e., the cytosol for a soluble second messenger like cAMP).

We consider a spherically shaped cell with radius $r = 5$ μm, placed in a chemoattractant concentration gradient causing a 60–40% linear gradient in receptor activity; i.e., 60% and 40% of the receptors are active at the front and back, respectively, or formally (see Methods): $\bar{R}^*_f = 0.6$, $\bar{R}^*_b = 0.4$, the mean fraction of active receptors $\bar{R}^* = 0.5$ and the difference from the mean $\Delta R^* = 0.1$.

The second-messenger gradient profile was analyzed for the three values of the diffusion coefficient D_m: 1, 10, and $100\ \mu m^2\ s^{-1}$, assuming a degradation rate of $k_{-1} = 1.0\ s^{-1}$, a maximum production rate $k_R = 1.0\ \mu Ms^{-1}$. The linear receptor gradient of 60–40% (Fig. 2, *dotted line*) then results in a linear second-messenger gradient of 59–41%, 55–45%, and 51–49% for the three values of D_m. In Eq 4, the slope of the second-messenger gradient relative to the gradient of active receptors is given by the factor F. Because the factor F is always smaller than 1, the resulting second-messenger gradient cannot be steeper than the gradient of receptor activity. As encountered already in the case of the

cylindrical model cell, only with a small space constant, i.e., a short dispersion range $\lambda \leq 1$ μm, the gradient in the external signal is transduced into an almost identical internal gradient of second messenger; fast diffusion or slow degradation will lead to a strong dispersion of the intracellular signal gradient. We conclude that slowly diffusing second messengers with $D_m < 1.0$ $\mu m^2 s^{-1}$ can preserve the external gradient, whereas fast-diffusing second messengers with $D_m > 100$ $\mu m^2 s^{-1}$ effectively generate an average global signal for realistic production and degradation rates.

A model for signal amplification with effector translocation

In the previous section, we have demonstrated that the second-messenger gradient will be always less steep than the gradient in receptor activity. *Dictyostelium* cells and neutrophils can respond to shallow chemoattractant gradients that are expected to induce a 12–10% gradient of receptor activation (Tomchik and Devreotes, 1981), indicating that amplification of the signal is essential. We develop a gradient amplification model that is based on translocation experiments of PH domain-containing proteins in *Dictyostelium* (Parent et al., 1998; Firtel and Chung, 2000), neutrophils (Servant et al., 2000), and fibroblasts (Haugh 2000). PH domains are known to bind to phosphatidyl inositol phosphates (see, for example, Rebecchi and Scarlata, 1998) that are generated upon receptor activation and possibly mediate the formation of transduction complexes (Parent and Devreotes, 1999). The diffusion coefficient of phosphatidyl inositol phosphates in living cells (about 1 $\mu m^2 s^{-1}$) allows gradient preservation at realistic degradation rates. To introduce a nonlinearity in the system, we assume that one essential component in the signal transduction cascade is a cytosolic PH-domain-containing protein that translocates between the cytosol and the second messenger in the plasma membrane. The principal is very general and can be achieved in two ways, both in respect to the identity of the second messenger in the membrane as the identity of the translocating molecule (see Discussion). Haugh et al. (2000) have proposed that PI3′-kinase may play such a role in signal localization. The model is depicted in four steps (Fig. 3): (*A*), before receptor stimulation only a small number of effector molecules is bound to the membrane and is inactive; (*B*), after receptor activation the membrane-bound effector molecules will be stimulated leading to production of small amounts of phospholipid second-messenger molecules; (*C*), because the phospholipid concentration increases, more effector molecules will translocate from the cytosol to the membrane; and (*D*), because the receptor now can signal to more effector molecules, this rapidly leads to stronger phospholipid production and further depletion of cytosolic effector molecules. The amplification can be considered as a positive feedback mechanism, where the phospholipid itself enhances its own production

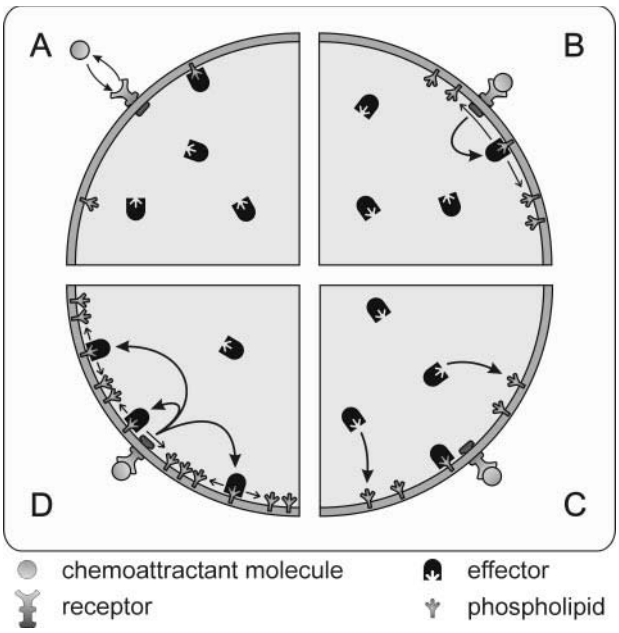

FIGURE 3 The diffusion–translocation model for amplification of signal transduction. The figure depicts four steps in the model: (*A*) receptor activation, (*B*) second-messenger production, (*C*) effector translocation, and (*D*) amplification.

by recruiting more effector molecules producing the phospholipid.

The production rate of second messenger, P, is directly coupled to the local receptor activity and the local effector enzyme concentration,

$$P(x) = k_0 + k_E R^*(x) E_m, \tag{5}$$

where k_0 is the basal phospholipid production rate, k_E is the maximum production rate per effector molecule, and E_m is the local effector concentration in the membrane. We further assume that effector molecules in the cytosol (E_c) are able to diffuse with diffusion coefficient D_{Ec}, and can reversibly bind to the phospholipids with forward binding-rate constant k_b and release-rate constant k_{-b}. The total amount of effector molecules in the membrane and the cytosol, E_{tot}, is held constant.

Amplification of a 60–40% external gradient

The concentration of effector molecule and second messenger were calculated with the translocation model using a linear gradient of receptor activity of 60–40%. The left panels of Fig. 4 show the concentration profiles of membrane-bound effector molecules, E_m, and cytosolic effector molecules, E_c, whereas the right panels show the cross-section of the cell; the gray scale indicates the local concentration of effector molecules. At 2 s after the application of the gradient, the cytosolic concentration of effector molecules has decreased to ~25 nM (Fig. 4 *B*), after 4 s to about

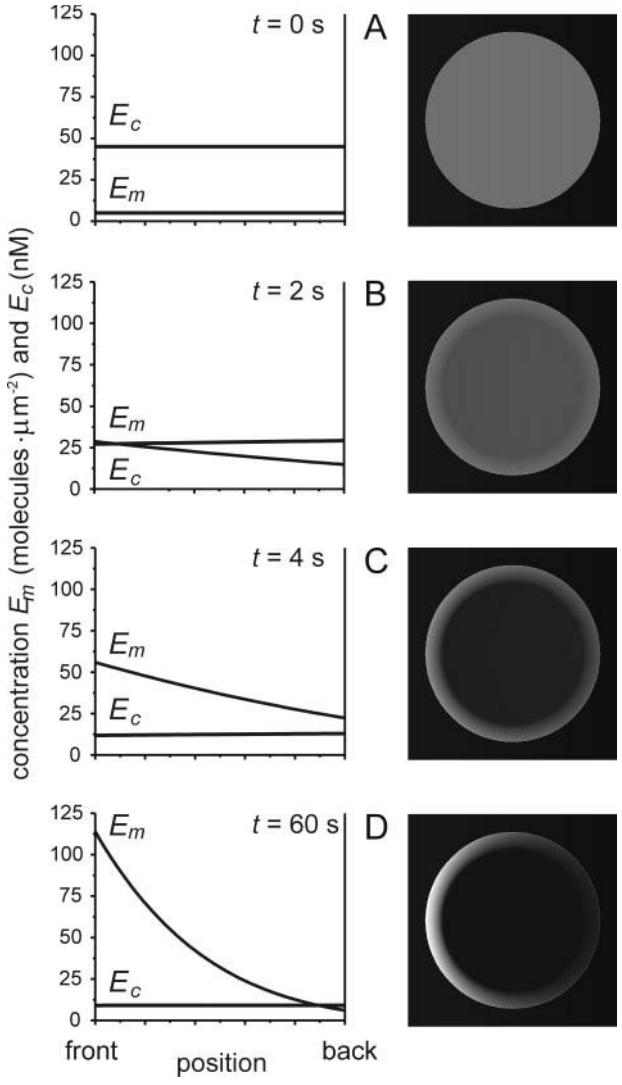

FIGURE 4 Translocation of effector from cytosol to membrane during gradient sensing with the diffusion–translocation model. Sequence of snapshots at four time points after application of a 60–40% gradient of receptor activity. The cytosolic and membrane-bound effector are depicted in two ways. The left-hand panels show the calculated values, where E_m is the density of effector molecules bound to the membrane and E_c the concentration of effector molecules in the cytosol. The panels at the right show the concentration of effector molecules at a cross section of the cell using a gray scale. The values for kinetic parameters used in the calculations are: $k_0 = 10$ molecules·μm^{-2} s^{-1}, $k_E = 20$ molecules·s^{-1}, $k_{-1} = 1.0$ s^{-1}, $k_b = 10$ μM^{-1} s^{-1}, $k_{-b} = 1.0$ s^{-1}, $D_{Ec} = 50$ μm^2 s^{-1}, and $D_m = 1.0$ μm^2 s^{-1}. The total concentration of effector molecules was taken to be 50 nM, and, before stimulation, ~10% of these effector molecules are bound to the membrane.

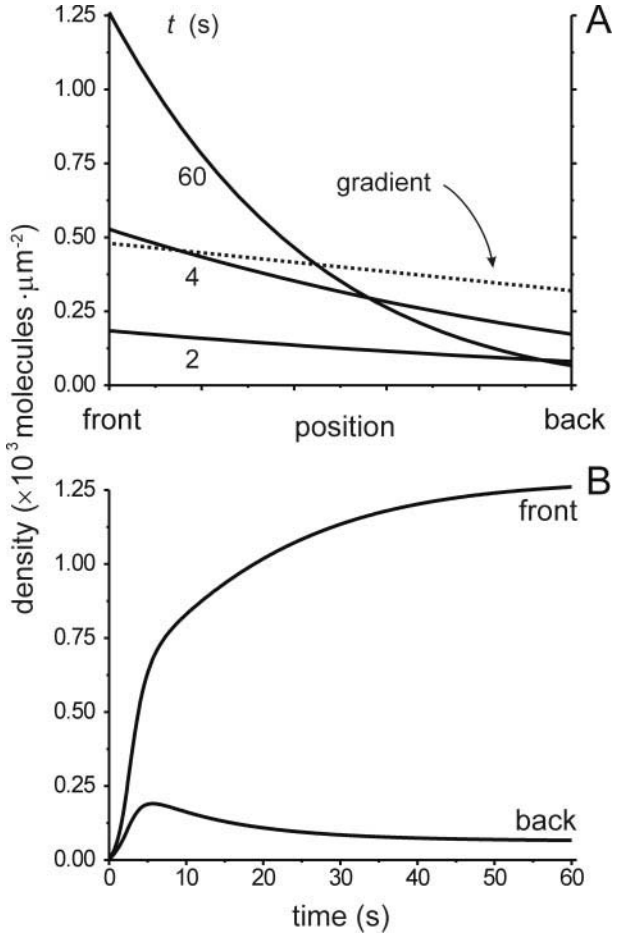

FIGURE 5 Second-messenger formation during gradient sensing with the diffusion–translocation model. (*A*) At $t = 0$, a gradient of 60–40% is applied to the cell. The dotted line depicts the steady-state second-messenger gradient if effector molecules would have been located at the membrane from the beginning (cf. Fig. 2). Black lines show the gradient calculated with the translocation model at three time points after application of the gradient. (*B*) Time courses of the concentration of second messenger at the front and at the back of the cell. See Fig. 4 for the parameter values.

10 nM (Fig. 4 *C*), which is followed by a slight further decrease to 8 nM, reached in the steady state (Fig. 4 *D*). This decrease is due to translocation of cytosolic molecules to phospholipid binding sites in the membrane that have been generated by effector molecules activated by receptors.

Whereas the effector molecules in the cytosol are spread evenly, those in the membrane are progressively concentrated at the front. Initially, during the first 2 s, the effector concentration in the membrane increases at all sides of the cell, and this increase is proportional to the 60–40% gradient of receptor activity. Later on, the membrane concentration of effector molecules increases further, however, this increase occurs more strongly at the front of the cell than at the back. In the steady state, reached after ~60 s, the effector concentration in the front is about 16-fold higher than in the back.

The concentration profiles of the phospholipid second-messenger molecules are presented in Fig. 5. The dotted line in Fig. 5 *A* represents the steady-state phospholipid concentration profile for a model without translocation (assuming that all effector molecules are distributed homogeneously in the membrane). In the translocation model, the second-messenger concentration gradient that is formed after 2 s

has a slope nearly identical to that of the gradient in receptor activity. At 4 s after application of the gradient, the concentration of second messenger has increased, which is stronger at the front of the cell than at the back. In the steady state, the second-messenger concentration has further increased at the front, but it has declined at the back of the cell.

The time course of the concentration at the front and the back of the cell is presented in Fig. 5 *B*. During the first second, the phospholipid concentration increases only slightly faster in the front than in the back of the cell, the difference being proportional to the difference in receptor activity at the front and back. Between about $t = 1–4$ s, the autocatalytic translocation process leads to an enhanced phospholipid production, but starts to saturate at $t = 4$ s, due to partial depletion of effector molecules in the cytosol. The enhanced amplification then levels off. In the second amplification phase, taking place between $t = 5–60$ s, the membrane-bound effector molecules gradually translocate from the back of the cell to the front. This leads to a decline of phospholipids in the back of the cell and a further increase frontally. The finally resulting 16-fold higher concentration of second messenger at the front is induced by only a 1.5-fold higher fraction of active receptors (i.e., a 60–40% gradient), and thus leads to an ~10-fold amplification, if compared to a model without translocation. The amplification process causes the second messenger production to be almost completely located at the front of the cell.

Amplification of signals at different receptor activity gradients

The receptor-stimulated production of phospholipids was investigated for different gradients in receptor activity (Fig. 6); i.e., gradients in receptor activity having different slopes or different mean activity, while applying the same settings of the kinetic parameters and diffusion coefficients as those used before. The case of the 60–40% gradient in the previous section is indicated by *point 1* in Fig. 6. Point 1 in Fig. 6, corresponding to a 52.5–47.5% gradient, results in a smaller difference in phospholipid concentration between the front and the back of the cell, yielding an amplification of 2.2 (*point 2*). For stronger gradients such as 75–25% receptor activity (*point 3*), this results in a strong amplification of ~34-fold, leading to a more than 100-fold gradient of phospholipid concentration over the cell length. All these gradients lead to a considerable depletion of the cytosolic effector concentration E_c from the initial 45 nM to ~10 nM.

With a 1.5-fold signal gradient at a lower mean receptor activity (15–10% gradient; *point 4*), the cytosolic effector concentration stays high, $E_c = 31.8$ nM, and the amplification is only 2.1-fold. For a 30–20% gradient (*point 5*), we obtain $E_c = 17.7$ nM and an amplification of 6.2, and for a 75–50% gradient (*point 6*) $E_c = 7.26$ nM and the amplification is 13.2. In general, it is observed that, at lower average receptor activity, amplification of the signal is smaller than at higher average receptor activity with the same receptor gradient. This is due to the limited depletion of the cytosolic effector molecules at lower receptor activity, which reduces the second amplification phase. Translocation of membrane bound effector from the back to front of the cell then hardly takes place.

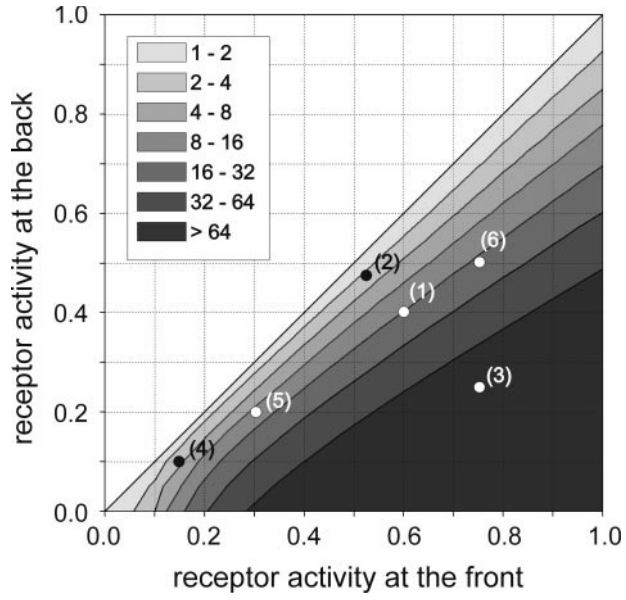

FIGURE 6 Contour-plot of gradient sensing. Ratio of second-messenger concentration, after 60 s, at the front and the back of the cell m_f/m_b, was calculated for different receptor activities at the front (R_f^*) and the back (R_b^*) of the cell. See Fig. 4 for the parameter values and see text for explanation of the marked points.

Improved gradient amplification at low receptor occupancy

At reduced average receptor occupancy, gradient amplification is less strong, mainly due to limited depletion of the cytosolic effector molecule. To improve gradient detection at low receptor occupance, the cell could increase second-messenger production per activated receptor. Biochemically, this can be achieved by increasing the amount of effector enzymes or by increasing the amount of second messengers produced per effector molecule (k_E). The second-messenger spatial concentration ratio (m_f/m_b) was calculated for different values of k_E: 20 (previous value), 100, and 200 molecules per effector. In all three cases, the receptor occupancy at the front of the cell is 1.5-fold higher than at the back of the cell. In Fig. 7 m_f/m_b is plotted against different average receptor occupancy ($\bar{R}^*$), demonstrating that amplification at low receptor occupancy is improved considerably by increasing the production rate of second messengers per activated receptor. Higher second-messenger production rates lead to higher second-messenger con-

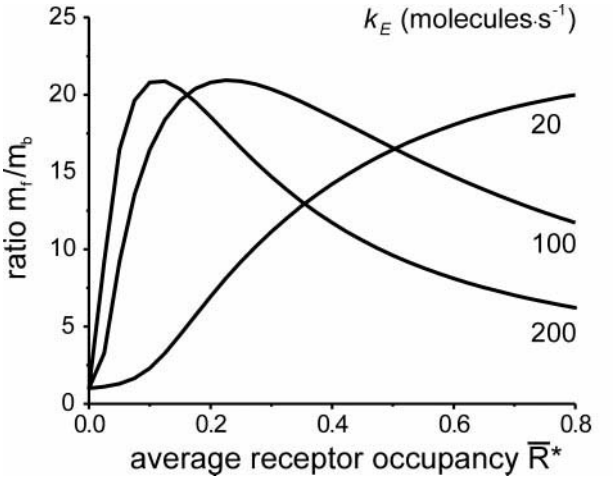

FIGURE 7 Amplification at low receptor occupancy. The steady-state ratio of second-messenger concentration at the front and the back of the cell m_f/m_b, was calculated for different average receptor activities. (R_f^*) and the back (R_b^*) of the cell. Enhancing depletion of the cytosolic effector molecule through higher production rates of second messenger improves amplification at low receptor occupancies.

centrations and hence more depletion. Figure 7 also reveals that, for $k_E = 100$ and $k_E = 200$, amplification declines at high receptor occupancy. Thus gradient detection can be improved at low receptor occupancy by increasing the expression of effector enzymes at the cost of reduced sensitivity at high signal concentrations.

Improved detection of very shallow gradients

Some cells are able to detect very shallow gradients of signal molecules that induce only a 1% gradient of receptor occupancy. To allow detection of such shallow gradients, a stronger amplification of the signal is essential. Here we assumed that, in addition to translocation of effector molecule E, also a cytosolic activator molecule A translocates to the membrane. Upon binding to the membrane, the activator stimulates production of second-messenger molecules.

The local production of second messengers then becomes

$$P(x) = k_0 + k_E R^*(x) E_m \frac{A_m}{A_m + K_A}, \qquad (6)$$

where A_m is the local activator concentration, and K_A is the concentration of activator molecules that gives half maximal active transduction complexes.

The receptor-stimulated second-messenger production with this two-component model was investigated for different gradients in receptor activity (Fig. 8 *A*); i.e., gradients in receptor activity having different slopes or different mean activity. The contour lines correspond to second-messenger concentration ratios between front and back (m_f/m_b) equal to 1, 10, and 100, where the number 1 means no amplification. In the plot, we can distinguish two very different areas

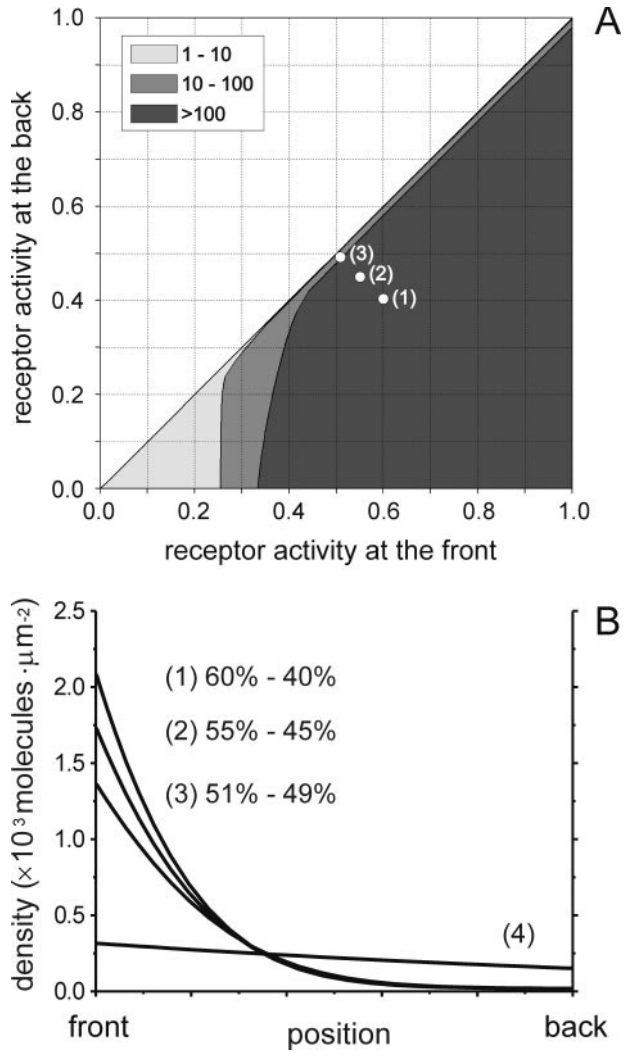

FIGURE 8 Contour-plot of gradient sensing using the effector–activator model. (*A*) The steady-state ratio of second-messenger concentration at the front and the back of the cell m_f/m_b, was calculated for different receptor activities at the front (R_f^*) and the back (R_b^*) of the cell. Parameter values used are: $k_0 = 10$ molecules·μm^{-2} s^{-1}, $k_E = 20$ molecules·s^{-1}, $k_{-1} = 1.0$ s^{-1}, for both effector and activator $k_b = 10$ μM^{-1} s^{-1}, $k_{-b} = 1.0$ s^{-1}, $K_m = 25$ molecules·μm^{-2}, $D_{Ec} = 50$ μm^2 s^{-1} and $D_m = 1.0$ μm^2 s^{-1}. The total concentration of effector and activator molecules was taken to be 50 nM. The model gives rise to a treshold concentration. Below this concentration no amplification occurs; above this concentration a strong activation at the front and strong inhibition at the back takes place. (*B*) Second-messengers gradients for the points indicated in panel A (*1*, *2*, and *3*). Amplification is very large and also occurs at small differences of receptor activity. Curve 4 was calculated with the same parameters as for curve 1, except that the diffusion coefficient was ten-fold larger ($D_m = 10.0$ μm^2 s^{-1}); the absence of a localized response indicates that the dispersion range of the second messenger must be very small.

of amplification. Up to ~25% receptor occupancy at the front of the cell, no strong amplification is observed. However, at higher receptor occupancy, a very strong all-or-nothing amplification of the signal takes place.

The second-messenger concentration profiles for three gradients of receptor occupancy are plotted in Fig. 8 *B*: (*1*)

40–60%, (*2*) 45–55%, and (*3*) 49–51%. The results demonstrate that, at the back of the cell, receptor-coupled second-messenger production is strongly inhibited, whereas at the front of the cell, second-messenger production is proportional to local receptor activity. A space–time analysis reveals how the two-component model leads to high sensitivity: Upon gradient stimulation of receptor activity, the second-messenger concentration increases faster at the front than at the back off the cell, by which it will reach earlier a critical threshold concentration. When this happens, the front will recruit very fast more activator and effector molecules, thereby strongly increasing second-messenger production, whereas at the back of the cell, second-messenger production is inhibited because the activator concentration in the cytosol will be below the threshold level.

The importance of the second-messenger diffusion constant, also for the two-component translocation model, is stressed by the second-messenger concentration profile indicated with (*4*) in Fig. 8 *B*. This curve corresponds to a calculation using a 60–40% receptor activity and a 10-fold higher second-messenger diffusion coefficient ($D_m = 10\ \mu m^2\ s^{-1}$), leaving all other parameter values the same. The response obtained is similar to the gradient of receptor activity. Thus, the dispersion range (λ) appears to be a very critical factor in the amplification mechanism and must be much smaller than the cell's length to allow effective transduction of chemical gradients.

DISCUSSION

Chemotactic gradient sensing requires transduction of the signal to the locomotion machinery of the cell. The intracellular messengers might be proteins and lipids in the membrane, or small molecules such as cAMP and proteins in the cytosol. In all cases, the diffusion of the second-messenger molecules has two pronounced effects, integration of receptor signals and communication to the locomotion system, but also dissipation of the spatial information. This dissipation can be reduced if the second-messenger molecule has a very short lifetime relative to its diffusion rate. If we consider the diffusion coefficients of various second-messenger molecules (see Table 1), it appears that small soluble second messengers diffuse very fast, by which they have a long range and a poor capacity to maintain localized responses. Only with a very high turnover, such second messengers are able to establish an intracellular spatial gradient. Molecules that diffuse very slowly, such as membrane proteins, have a very short range, even when their degradation/inactivation is relatively slow. Although these molecules can establish very steep gradients, diffusion and communication to other parts of the cell is extremely slow, taking several minutes. A 10-μm cell that responds to chemotactic signals after ~5 s therefore presumably relies on second messengers diffusing a few micrometers in a few seconds and having a turnover of a few seconds. Membrane lipids have diffusion coefficients of ~1 $\mu m^2\ s^{-1}$ and thus fulfil that expectation. A similar conclusion, based on experimental data, was reached by Haugh et al. (2000).

TABLE 1 Dispersion of different second messengers

Second messenger	Diffusion coefficient D_m ($\mu m^2\ s^{-1}$)	Dispersion Range* λ (μm)	Dispersion Time† τ_1 (s)
cAMP in cytosol	>100	>10	~0.1
Protein in cytosol	10–50	~5	~0.25
Lipid in membrane	1	1	~1
Protein in membrane	~0.1	~0.3	~1

All values were calculated with $k_{-1} = 1.0\ s^{-1}$.
*About 95% of the molecules are localized within a distance of 3λ from the source.
†After λ_1 seconds, the concentration has reached 63% of the steady-state value.

Detection of a gradient with linear signal transduction can never produce a second-messenger gradient that is steeper than that of the applied signal. Because many organisms can detect very small gradients at a low average receptor activity, a locally strong amplification is essential to generate an all-or-nothing locomotion response. Meinhardt (1999) and Meinhardt and Gierer (2000) have put forward a model that explains gradient sensing by combining strong local autocatalytic activation with global inhibition, by which the net activity at the front becomes much higher than in the back. Calculations have shown that this model provides the required nonlinear amplification, but the model is biochemically rather complex and is sensitive to the parameter set chosen. The model of Parent and Devreotes (1999) incorporates adaptation of the local stimulatory and global inhibitory responses to constant signals, by which the net amplification at the front becomes strongly enhanced. The present diffusion–translocation model does not incorporate any of these mechanisms except for a positive feedback on second-messenger production, and still is very robust in generating strong local responses. Nevertheless, incorporation of global inhibition and adaptation expands the applicability of the present model to more extreme situations such as rapid reversal of the gradient (unpublished results).

The diffusion–translocation model

The heart of the diffusion–translocation model is that activation of the chemoattractant receptor results in the creation of membrane-bound second-messenger molecules. The second messengers then act as docking sites for effector molecules in the cytosol that mediate (or facilitate) the transmission of the signal from the active receptor to the second-messenger-producing enzyme. The transduction cascade thus contains a positive feedback loop that strongly and nonlinearly amplifies the signal. The amplification saturates when the cytosolic pool of molecules becomes partially depleted.

The membrane-bound second messenger could be any lipid or protein that functions as (or induces) a docking sites for cytosolic proteins. Thus, phosphatidyl inositol polyphosphates that are generated by receptor-stimulated kinases may form binding sites for proteins with specific PH domains. Alternatively, receptor-stimulated protein tyrosin phosphorylation can form binding sites for proteins with SH2 domains. Possible candidates for the effector enzymes that mediate second-messenger formation are heterotrimeric G-protein subunits, small G-proteins, or a protein kinase that activates a membrane-bound effector enzyme through phosphorylation.

In its most simplified form, the second messenger is a phospholipid, and the translocating component is the phospholipid-forming enzyme. We will discuss the model with this simplified form in mind. The combined data of Figs. 4 and 5 reveal that a small spatial difference in receptor activity is transduced into a phospholipid second-messenger concentration gradient that initially has the same slope as the gradient of receptor activity. Because the produced phospholipid molecules are the binding sites for the effector enzyme, slightly more effector enzymes translocate to the front than to the back of the cell. The increased effector concentration at the front of the cell leads to a more pronounced phospholipid production, and, subsequently, to a depletion of the effector enzyme in the cytosol. In the second phase of amplification, the membrane-bound effector enzymes dissociate at the back of the cell and gradually translocate to the front. As a consequence, the phospholipid second-messenger concentration further increases at the front and decreases appreciably at the back of the cell. Gradient amplification is achieved because second-messenger production becomes almost completely restricted to the front of the cell. Effectively, the production point source situation as described in the results section is obtained in this way, and hence the corresponding requirements for gradient formations apply. The main factor is the dispersion range of the second messenger, which must be in the order of 1 μm for small chemotactic cells.

Limitations and improvements of the model

The two phases of amplification in the diffusion–translocation model entail different mechanisms that cause both limitations and enable improvements of the model. Amplification requires time, during which dispersion will take place that reduces amplification. Therefore, amplification should occur within the dispersion time. Because amplification is mainly determined by translocation of the cytosolic effector enzyme, this implies that its translocation speed must be faster than the dispersion of the second messenger. With the diffusion speeds of a cytosolic protein as the effector enzyme and a membrane phospholipid as the second messenger, this condition is easily fulfilled. Dispersion of the second messenger can be reduced either by reducing diffusion speed or by increasing the degradation rate of the second messenger. Thus, simply by increasing the expression level of degrading enzymes, the second-messenger gradient will become steeper. Slower second-messenger diffusion can be achieved by either restricted diffusion (corralled and percolation) or by protein-bound second messengers. It has been demonstrated that, in *Dictyostelium*, signals adapt, meaning that, under persistent stimulation, the intracellular signal returns to basal levels, which implies that, after the initial activation, some form of inhibition takes place. This phenomenon has not been included in the model. However, it will enhance the localization process if adaptation occurs faster at the side of lower activity, thereby amplifying the localization of second messenger in areas with higher activity (unpublished results).

The sensitivity of gradient sensing consists of two components, the detection of gradients at low concentrations and the detection of shallow gradients. At low receptor activity, amplification is predominantly determined by basal production activities and the second amplification phase is absent, because there is no significant depletion of the cytosolic effector enzyme. Thus, at receptor activities below $\sim$10%, amplification of the gradient becomes small. This has the advantage that the system does not become unstable at low receptor activities, which is a general problem of highly nonlinear systems at low activity. Our calculations demonstrate that sensitivity at low average receptor activity can be improved simply by increasing the amount of second messengers produced per activated receptor, which leads to stronger depletion of the cytosolic effector. Biochemically, this would mean that a cell can enhance the detection limit of gradient sensing by increasing the expression of one of the components of the signal transduction cascade. In the basic model, only one component of the signaling transduction pathway translocates to the membrane, leading already to considerable signal localization. Some cells are able to respond to very shallow chemotactic gradients. When assuming that more components translocate to the second messenger in the membrane, thereby forming activated transduction complexes, second-messenger production can virtually completely be restricted to one side of the cell, even for minor gradients. Interestingly, such a two-component translocation model reveals a threshold of receptor activity below which nonlinear amplification is very limited. This has the important advantage that, at low receptor activity, the system is relatively silent and stable. As for the one-component translocation model, the threshold can be reduced to lower receptor activity by increasing the amount of second-messenger molecules produced per activated receptor. Thus, cells become sensitive to small and shallow gradients by inducing the expression of a co-activator and by enhancing the expression of an existing component of the signal transduction cascade. Such more complicated and stronger nonlinear mechanisms can, however, lead to freezing of the intracellular signal, because multiple steady-state

concentration profiles may exist. In contrast to the one-component model, reversal of the external gradient signal then may not lead to reversal of the internal gradient. A similar very high sensitivity, but tendency for freezing of the second-messenger gradient, was observed upon incorporating global inhibition and local activation into the translocation model. Preliminary work indicates that introducing exact adaptation mechanisms, where internal signals are only temporarily maintained, can solve this freezing problem.

The diffusion–translocation mechanism presented here may very well form the central unit of signal transduction processes in which spatial information has to be transduced. On top of this unit, other biochemical modules, such as adaptation or inhibition mechanisms, may fine-tune the model such that it becomes increasingly sensitive and applicable for more complicated spatial signals such as gastrulation, and mesoderm induction.

We thank D. G. Stavenga and J. Roelofs for stimulating discussions and critically reading of the manuscript.

REFERENCES

Allbritton, N. L., T. Meyer, and L. Stryer. 1992. Range of messenger action of calcium ion and inositol 1,4,5-trisphosphate. *Science.* 258: 1812–1815.

Almeida, P. F. F., and W. L. C. Vaz. 1995. Lateral Diffusion in Membranes. Elsevier, Amsterdam. 305–357.

Arrio-Dupont, M., G. Foucault, M. Vacher, P. F. Devaux, and S. Cribier. 2000. Translational diffusion of globular proteins in the cytoplasm of cultured muscle cells. *Biophys. J.* 78:901–907.

Carslaw, H. S., and J. C. Jaeger. 1959. Conduction of Heat in Solids. Clarendon Press, Oxford, UK.

Chen, C., T. Nakamura, and Y. Koutalos. 1999. Cyclic AMP diffusion coefficient in frog olfactory cilia. *Biophys. J.* 76:2861–2867.

Crank, J. 1979. The Mathematics of Diffusion. Clarendon Press, Oxford, UK.

Devreotes, P. N., and S. H. Zigmond. 1988. Chemotaxis in eukaryotic cells: a focus on leukocytes and Dictyostelium. *Annu. Rev. Cell Biol.* 4:649–686.

Firtel, R. A., and C. Y. Chung. 2000. The molecular genetics of chemotaxis: sensing and responding to chemoattractant gradients. *Bioessays.* 22:603–615.

Haugh, J. M., F. Codazzi, M. Teruel, and T. Meyer. 2000. Spatial sensing in fibroblasts mediated by 3′ phosphoinositides. *J. Cell Biol.* 151: 1269–1280.

Haugh, J. M., and D. A. Lauffenburger. 1997. Physical modulation of intracellular signaling processes by locational regulation. *Biophys. J.* 72:2014–2031.

Heldin, C. H., and B. Westermark. 1999. Mechanism of action and in vivo role of platelet-derived growth factor. *Physiol. Rev.* 79:1283–1316.

Korlach, J., P. Schwille, W. W. Webb, and G. W. Feigenson. 1999. Characterization of lipid bilayer phases by confocal microscopy and fluorescence correlation spectroscopy. *Proc. Natl. Acad. Sci. U.S.A.* 96:8461–8466. [Published erratum. *Proc. Natl. Acad. Sci. U.S.A.* 1999. 96:9666].

Meinhardt, H. 1999. Orientation of chemotactic cells and growth cones: models and mechanisms. *J. Cell Sci.* 112:2867–2874.

Meinhardt, H., and A. Gierer. 2000. Pattern formation by local self-activation and lateral inhibition. *Bioessays.* 22:753–760.

Niv, H., O. Gutman, Y. I. Henis, and Y. Kloog. 1999. Membrane interactions of a constitutively active GFP-Ki-Ras 4B and their role in signaling. Evidence from lateral mobility studies. *J. Biol. Chem.* 274: 1606–1613.

Parent, C. A., B. J. Blacklock, W. M. Froehlich, D. B. Murphy, and P. N. Devreotes. 1998. G protein signaling events are activated at the leading edge of chemotactic cells. *Cell.* 95:81–91.

Parent, C. A., and P. N. Devreotes. 1999. A cell's sense of direction. *Science.* 284:765–770.

Rebecchi, M. J., and S. Scarlata. 1998. Pleckstrin homology domains: a common fold with diverse functions. *Annu. Rev. Biophys. Biomol. Struct.* 27:503–528.

Servant, G., O. D. Weiner, P. Herzmark, T. Balla, J. W. Sedat, and H. R. Bourne. 2000. Polarization of chemoattractant receptor signaling during neutrophil chemotaxis [see Comments]. *Science.* 287:1037–1040.

Stock, A. M., and S. L. Mowbray. 1995. Bacterial chemotaxis: a field in motion. *Curr. Opin. Struct. Biol.* 5:744–751.

Stock, J. B., A. J. Ninfa, and A. M. Stock. 1989. Protein phosphorylation and regulation of adaptive responses in bacteria. *Microbiol. Rev.* 53: 450–490.

Teruel, M. N., and T. Meyer. 2000. Translocation and reversible localization of signaling proteins: a dynamic future for signal transduction. *Cell.* 103:181–184

Tomchik, K. J., and P. N. Devreotes. 1981. Adenosine 3′,5′-monophosphate waves in *Dictyostelium discoideum*: a demonstration by isotope dilution–fluorography. *Science.* 212:443–446.

Xiao, Z., N. Zhang, D. B. Murphy, and P. N. Devreotes. 1997. Dynamic distribution of chemoattractant receptors in living cells during chemotaxis and persistent stimulation. *J. Cell Biol.* 139:365–374.